SPECIAL ISSUE

Bima Journal of Science and Technology, Vol. 7 (2.1) August, 2023 ISSN: 2536-6041

CHARACTERIZATION OF HETEROGENOUS CATALYST PRODUCED BY PHYSICAL ACTIVATION OF *Cocos nucifera* SHELL WASTE

MIKYITSABU AGO ATOSHI and JOHNSON GANI

Department of Chemical Sciences, Federal University Wukari, Taraba State, Nigeria.
Corresponding Author: agomikyi@gmail.com

ABSTRACT

Heterogeneous catalytic transesterification has several advantages over the homogeneous catalytic transesterification, including easy separation of biodiesel from glycerol, catalyst recycling/reuse, less energy requirement, and minimum consumption of water. In this study, the effect of temperature on the percentage yield of catalyst produced, effect of pH, Fourier Transform Infrared analysis, morphology, ash content, moisture of catalyst produced by both physical and chemical activation of *Cocos nucifera* shell was studied. The spectra for *Cocos nucifera* shell catalyst, shows different spectra at different wavelengths of 3339.7cm^{-1}, 2885cm^{-1}, 1684cm^{-1}, 1581.8cm^{-1}, 1151.7cm^{-1}, and 745.5cm^{-1}. 3339.7cm^{-1} associated to O-H stretching vibration of OH functional groups. Gradual decrease with increase in the concentration of K_2CO_3, optimum yield was observed at 1:6 with total yield of 76.30%. The effect of activation temperature increases the ash content of the catalyst from 500 to 700^{o}C leading to a gradual increase in ash content from 5.4 to 9.6. Moisture content of the catalyst produced at different activation temperatures and impregnation ratios was found to decrease with increase in activation temperatures, and increase with increase in impregnation ratio. Catalyst produced at higher activation temperature 700 to 900^{o}C show a lower moisture content of 5.4 and 3.2% respectively. This work concludes that, Heterogenous catalyst can be produced from *Coco nucifera* shell which is an agricultural waste and can be further used as catalyst for biodiesel.

Keywords: *Activation, catalyst, Coco nucifera, shell, waste*

INTRODUCTION

Coco nucifera is mainly composed of lignin, cellulose and hemicelluloses (Borel *et al.,* 2021). Increasing the rate of cellulose breakdown improves the porous structure of biochar (Li *et al.,* 2020), whereas increasing the rate of lignin breakdown contributes to the formation of biochar with a high specific area, high FC content and fine aromatic structure (Jiang *et al.*, 2020). The composition of lignin, cellulose and hemicellulose in a *Cocos nucifera* shell influences the characteristics of *Cocos nucifera* shell. Kamaluddeen *et al.* (2022) studied the production of solid catalyst from carbonaceous materials. This requires careful approach so that the physical or mechanical properties of all intermediates are not destroyed. Filtration, drying, calcination, and forming rather than the batch method are recommended.

Dass *et al.* (2018) studied the morphology of catalyst produced from *Coco nucifera* fruit shells by physical activation at 900°C. Cavities were visible on the surface of the catalyst of different sizes. The different pores suggest that these could be sites that may adsorb reactants during catalysis (Jiang & Xiao, 2020). Also, the size of the pore could be related to the different functional groups that may be present (Lee et al., 2019). The nature of functional group on catalyst surface has been related to the nature of reaction that would proceed in heterogeneous catalysis

(Charlotte and Bert, 2022). This work focuses on producing a heterogenous catalyst from *Coco nucifera* shell and evaluation of heterogenous catalyst produced by physical activation from *coco nucifera* shell

MATERIALS AND METHODS

Methods

The *Cocos nucifera* shells were collected from coconut sellers in Wukari LGA, Taraba State. The *Cocos nucifera* shell were washed with tap water, sun-dried for two days and crushed to small particle size. A 500g of crushed *Cocos nucifera* shell was washed with distilled water till the wash water became colorless. It was then dried at 110°C in an oven for 8 hours to get rid of moisture and other volatiles.

Physical activation: A 100g of pre-treated *Cocos nucifera* shell was carbonized in a crucible and at 1000°C for 2 hours. After carbonizing for 2 hours, the sample was kept in a desiccator to cool. It was ground and sieved with a 300µm sieve and Storage in air tight bottle to avoid long contact with oxygen.

Determination of the percentage yield of Catalyst produced by physical activation (K_2CO_3 cm^3) of *Cocos nucifera* shell

The total yield (%) of *Cocos nucifera* shell produced by physical activation was determined after sample processing in terms of raw material mass. The dried weight, of the pre-treated and carbonized samples was determined using Metler balance and the carbon yield and calculated as

$$Y\% = \frac{W\ x\ 100}{W°} ----- Eq\ 1$$

Where Y = Carbon yield (%); W = final weight of catalyst prepared; W° = initial weight of the sample used in the carbonization and activation processes (Verla *et al*., 2012).

Determination of pH of catalyst produced by physical activation of *Cocos nucifera* shell

The pH was determined according to ASTM D3838-80 1.0g of each of the catalysts produced by physical activation of *Cocos nucifera* shell was weighed and transferred into separate 250 ml beaker and 100 ml of distilled water was added and stirred for 1 hour. The samples were allowed to stabilize and then the pH was measured using a hand-held pH meter, (Jenway 430 Model).

Determination of percentage Ash content of the produced catalyst

Ash content determination was done according to the ASTM D2866-94 method. 2g of each of *Cocos nucifera* shell catalyst was placed into separate porcelain crucible which was weighed and transferred into a preheated muffle furnace set at a temperature of 1000°C. The furnace was allowed to burned for an hour after which the crucible and its content was transferred to a desiccator and allowed to cool. The crucible and content were reweighed and the weight lost was recorded as the ash content of the catalyst (W_{ash}) and the % ash content (dry basis) was calculated from the equation (Verla *et al*., 2012).

$$Ash\ = \frac{Wash\ X\ 100}{W°} ----- Eq\ 2$$

W^o = initial weight of AC, W_{ash} = weight loss

Moisture (%) of catalyst produced

Moisture content was determined according to ASTM D2867-99. From the Catalyst produced, 1g was weighed and dried in an oven set at 110°C. The drying sample was constantly weighed at a 10 minutes' interval until a constant weight ($W_{p)}$ was obtained. The crucible and its content were retrieved and cooled in desiccator. The difference in weight was recorded and the moisture content (MC) was calculated from the equation as loss in

weight on drying divided by initial weight of activated carbon multiplied by 100. (Donni *et al*., 2005).

$$MC = \frac{Wf - Wi \ X\ 100}{\text{Wo}} \quad ---- \ Eq\ 3$$

Where Wf = weight of Carbon retrieved from the oven, Wi = weight of crucible and AC and W_o = initial dry weight of the AC sample

The morphological studies of the catalyst Oven dried porous sample was mounted on an adhesive carbon tape attached to an aluminium-stub and subsequently sputter coated with platinum for 5 min in a JFC-1100 sputter coater. SEM magnification was selected at 370, 500, 1000 and 1500 (Guo *et al.,* 2010). Scanning Electron Microscope (SEM) operating at 25 kV was used to study the morphology.

Fourier Transform Infrared analysis of catalyst

Catalyst was analyzed was using a PERKIN-ELMER spectrum One FT-IR spectrophotometer. Each sample was ground to fine powder and oven dried at 11°C for 2 hours and turned into pellet hydrolytically. The pellet was analyzed immediately and the spectra produced was recorded. A pellet prepared with an equivalent quantity of pure KBr powder was used as control (Sugumaran *et al.,* 2012).

RESULTS AND DISCUSSIONS

Effect of temperature and impregnation ratio Proximate analysis as shown in Table 1, these are the different properties of catalyst produced by physical activation of *Cocos nucifera* shell. As seen from the results, carbonization temperature has effect on the yield as *Cocos nucifera* precursor reduces upon carbonization at 1000ºC this indicates that coconut shell was practically sensitive to the carbonization temperature. The effect of increasing the reaction temperature and impregnation ratio shows a gradual decrease in the yield (Fig.1), optimum temperature was found to be 800ºC which yields 78.33%.

Table 1: Proximate analyses of catalyst produced from *Cocos nucifera* shell

Parameter	Catalyst produced
Catalyst yield (%)	52.37
pH of catalyst	9.70
Percentage ash (%) of catalyst	2.01
Percentage moisture (%) of catalyst	2.80

Effect of Temperature (ºC) On the Yield (%) of *Cocos nucifera* Shell Catalyst.

Figure 1: shows the effect of temperature on the yield (%) of the carbonized *Cocos nucifera* shell when the temperature was varied from 500 to 900 ºC at between constant concentration of catalyst and time, the result shows that the yield of catalyst decreases gradually as the temperature increases from 500 to 700ºC and there was a decrease in catalyst yield from 700 to 900ºC also. The optimum yield of the *Cocos nucifera* Shell Catalyst observed at 500ºC was 85.33%.

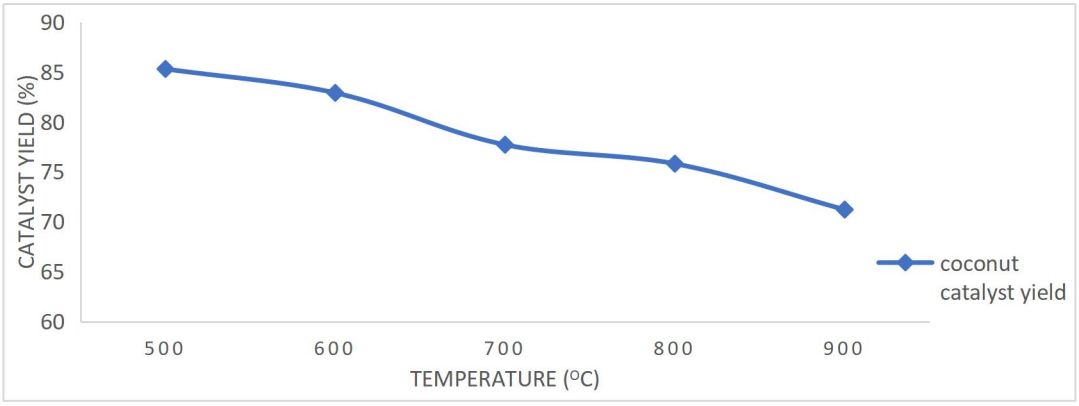

Figure 1: Effect of temperature on catalyst yield at constant impregnation ratio (gdm^3) and time

Impregnation ratio K_2CO_3 (gdm^{-3}) on the yield of Cocos nucifera shell Catalyst.

Figure 2: The impregnation ratio was varied from 3:2 to 3:10 of K_2CO_3 and the *Cocos nucifera* shell. As the impregnation ratio was increased at constant temperature and time on the carbonized *Cocos nucifera* shell, the catalyst yield decreases progressively as the impregnation ratio increases from 2 to 10 gdm^{-3}. At 8 to 10 gdm^{-3}, there was a minimal decrease in the yield of both the *Cocos nucifera* catalyst with the highest yield observed at 3: 2 with 86.63% yield. The effect of varying impregnation ratio of catalyst prepared by physical activation to potassium carbonate (K_2CO_3) at constant temperature and time, the result obtained showed a gradual decrease with an increase in the concentration of K_2CO_3. Optimum yield was observed at 1:6 (catalyst: K_2CO_3) with total yield of 76.30%. The catalyst exhibits an alkaline nature for all the catalyst prepared at different activation temperature and impregnation ratio, at 800°C with impregnation ratio of 3:6 K_2CO_3.

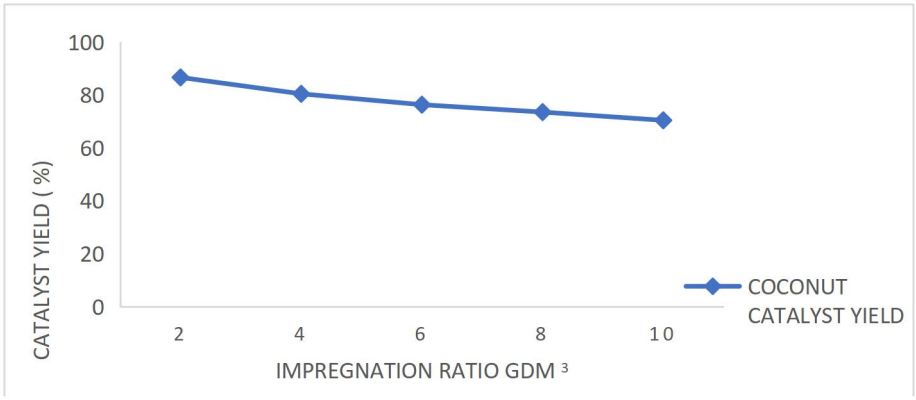

Figure 2: Effect of impregnation ratio (gdm^3) on catalyst yield at constant temperature (°C)

Effect of temperature variation on pH of catalyst

Figure 3: shows the pH of catalyst from carbonized *Cocos nucifera* shell at constant impregnation of K_2CO_3 and time. As the temperature of the reaction increases the pH increases from 9.2 to 10.8. This shows the alkalinity of the catalyst. The optimum temperature for carbonization was observed at 800°C with pH of 10.4. The pH of the catalyst

was found to be 10.5. The value of pH obtained in this work is more effective because pH of catalyst obtained from lignocellulosic material is very effective at low pH than high pH (Edward *et al.,* 2014).

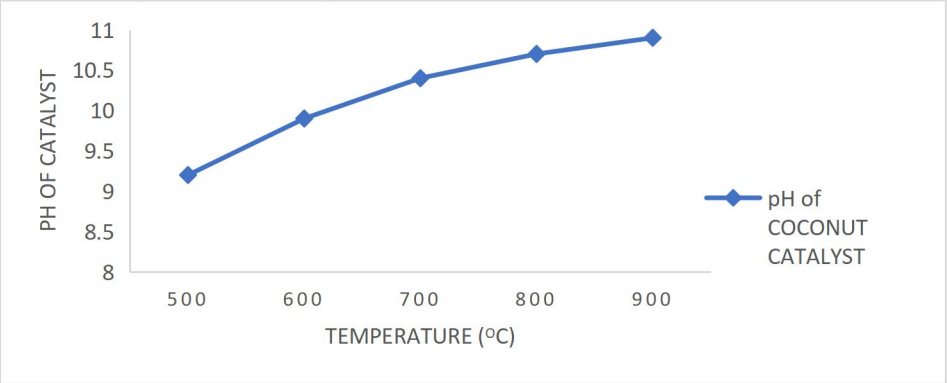

Figure 3: Effect of temperature variation on pH of catalyst at constant impregnation ratio (gdm^3) and time

Effect of various impregnation ratio (gdm^{-3}) of K_2CO_3 on pH of the catalyst

Figure 4: from the results it shows that the pH of catalyst increases with increasing concentration of K_2CO_3 this shows an increasing alkalinity of the catalyst. There was a minimal increase from 2 to 4 gdm^{-3}. The optimum pH was observed to be 10.5 at 3:6.

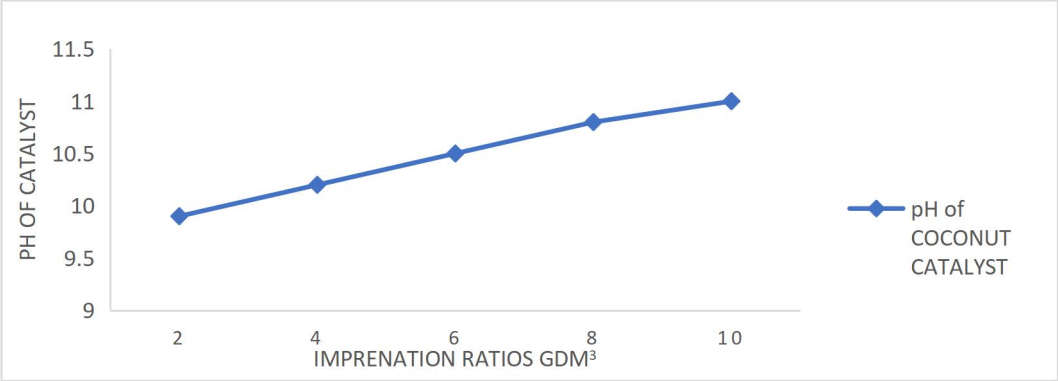

Figure 4: effect of various impregnation ratio (gdm^3) on pH of catalyst at constant temperature (°C) and time

Impact of temperature variation on ash content of the catalyst

Figure 5, shows the ash content of *Cocos nucifera* shell catalyst which was activated at different temperature range and constant concentration of K_2CO_3 and time. The effect of activation temperature increases the ash content of catalyst in both coconut shell and mahogany shell catalyst at 1000°C, catalyst activated at 500 to 700°C shows a gradual increase in ash content from 5.4 to 9.6 and as the temperature increases from 700 to 900°C the ash content increases 9.6 to 13.2 for *Cocos nucifera* shell catalyst, as the temperature increases from 700 to 900 °C the ash content was observed to be 11.2 to 15.3. The catalyst shows a lower ash content. High ash content is undesirable for catalyst since it reduces the mechanical strength of catalyst.

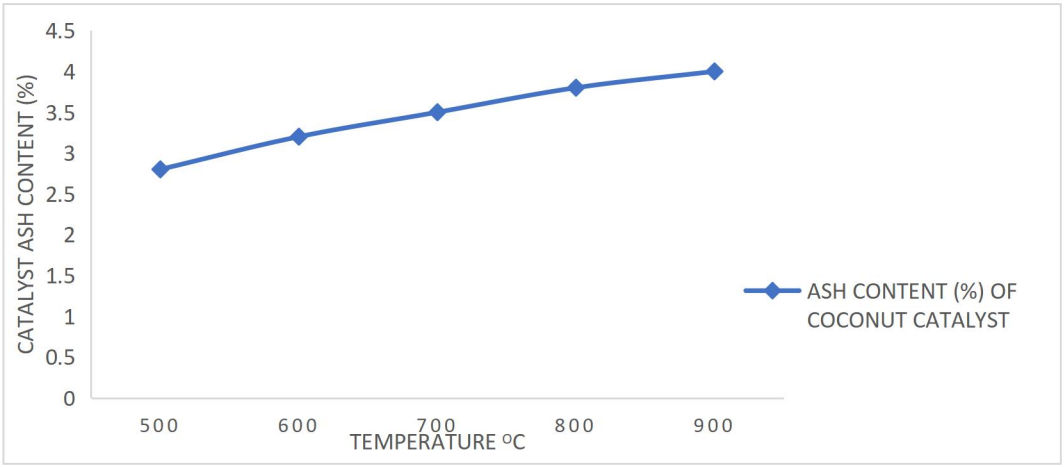

Figure 5: Growth trend of ash content of the catalyst under various temperature at constant impregnation and time

Impact of the variation of impregnation ratio on ash content of the catalyst

Figure 6: shows an increasing ash content with increasing impregnation ratio. The highest percentage ash for *Cocos nucifera* shell catalyst was observed at 3:10 with 14.8%.

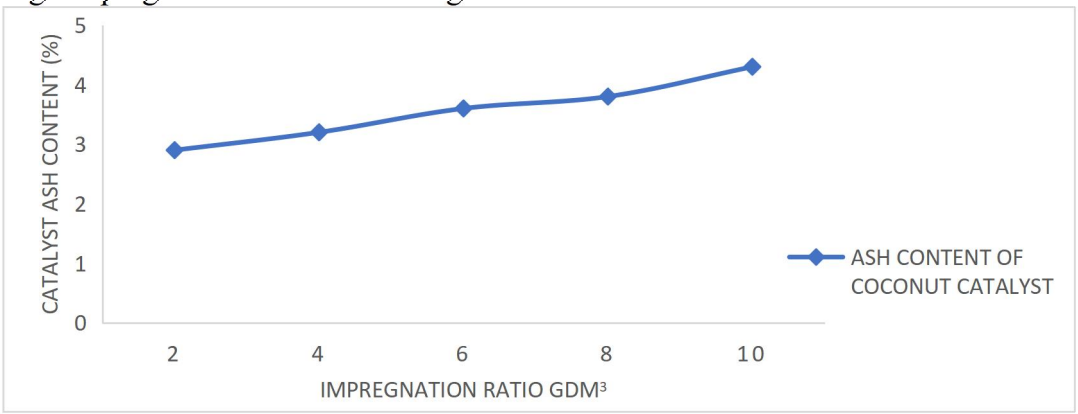

Figure 6: Growth trend of ash content of the catalyst under various impregnation ratio

Moisture Content (%) of Catalyst at Different Reaction Temperature.

Figure 7: At different reaction temperature, the moisture content of *Cocos nucifera* shell catalyst shows a significant decrease in moisture content with the lowest moisture content at 900°C with 3.2 % and the highest was 8.9 % at 500°C.

Figure 8: shows a gradual increase in moisture content as the impregnation ratio increases from 2 to 10 gdm^3. Moisture content increases from 5.6 to 9.0% in the coconut shell catalyst and 4.8 to 8.9 in *Cocos nucifera* shell Catalyst. The moisture content of the catalyst produced at different activation temperatures and impregnation ratios was found to decrease with an increase in activation temperatures and increase with an increase in impregnation ratio, catalyst produced at higher activation temperature 700 to 900°C show a lower moisture content of 5.4 and 3.2% respectively. Lower moisture content increases the rate of adsorption.

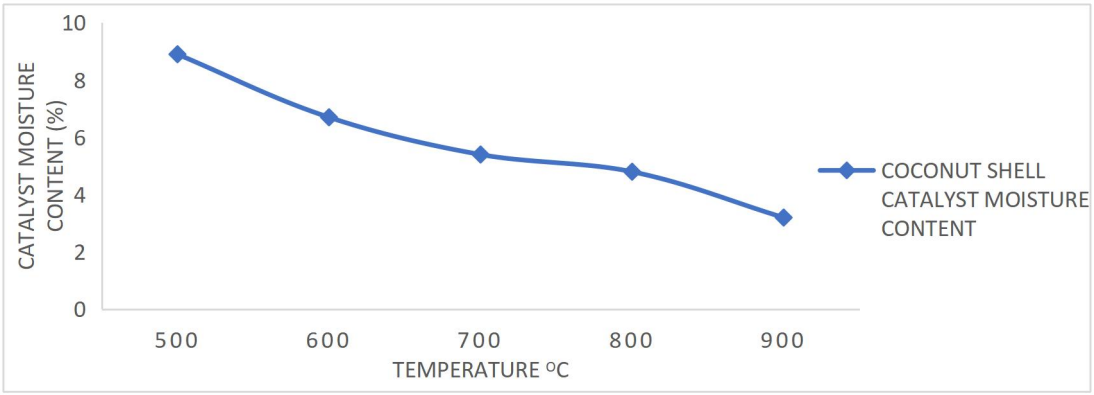

Figure 7: Moisture content of catalyst under different reaction temperature (°C) at constant impregnation ratio (gdm^3) and time (h).

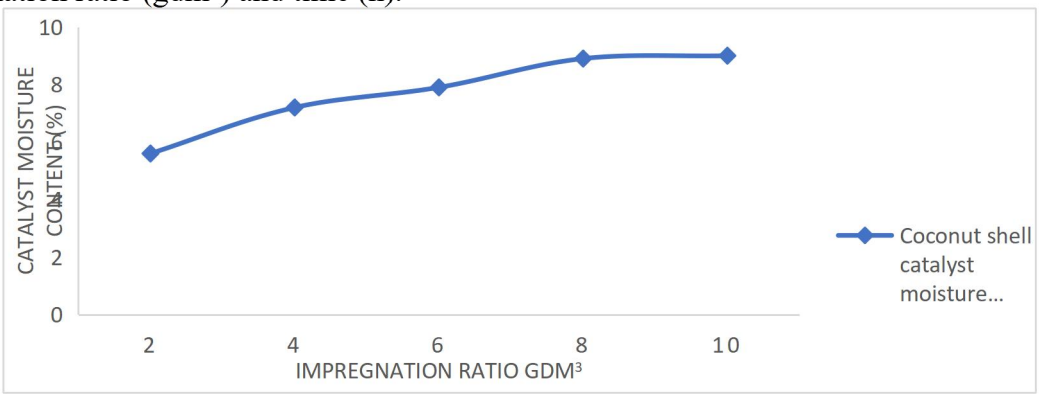

Figure 8: Moisture content of catalyst at different impregnation ratio (gdm^3), constant reaction temperature (°C) and time (h).

Morphological characterization of *Cocos nucifera* Shell Catalyst

Figure 9 and 10 shows the different morphology of physically prepared *Cocos nucifera* shell activated carbon, coconut shell catalyst produced at 800°C and 3:6 K_2CO_3 impregnation ratio. From the micrographs, it can be seen that the external surface of the carbon has some pores on the surface which indicates the porosity of activated carbon. Figure 14 shows the morphology of *Cocos nucifera* shell catalyst chemically prepared at 800°C from the scanned result, the external surface developed some cracks, crevices of honeycomb-like structure and some crystals and strands with pores scattered on the surface of the carbon. A closer look shows some pores developed on the crystals. The crystals formed on the surface are most likely the potassium compound as is hinted out by the result of the scan (Eliseo *et al.,* 2015).

Bima Journal of Science and Technology, Vol. 7 (2.1) August, 2023 ISSN: 2536-6041

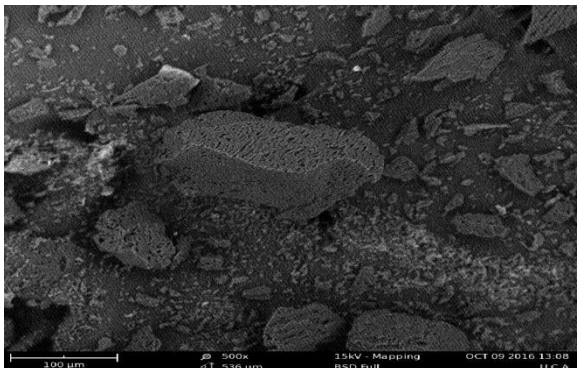

Figure 9: SEM for physically prepared *Cocos*. shell *nucifera* shell catalyst

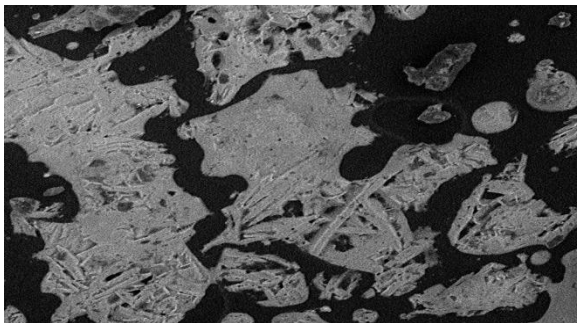

Figure 10: SEM result for *Cocos nucifera* catalyst produced at 800ºC.

Coconut Shell Catalyst Produced at Different Activation Temperatures ºC.

Fourier transform infrared (FTIR) spectroscopic analysis was used to study the surface chemistry of both physically and chemically prepared coconut shell catalyst. Figure 11 and 12 reveal the FTIR spectra of the *Cocos nucifera* shell catalyst where the peaks were slightly shifted. Figure 11 shows the spectra of physically produced *Cocos nucifera* shell catalyst with varying peaks of 3339.7cm-1 which is associated with -OH stretching, 2885.0cm-1 which corresponds to C-C stretch, weak peak at 1684.8 corresponds to C=C stretch, C=O was found at 1581.8, at 1151.7 corresponds to the stretching vibration of C-O and at 745.5cm-1 C-H was found.

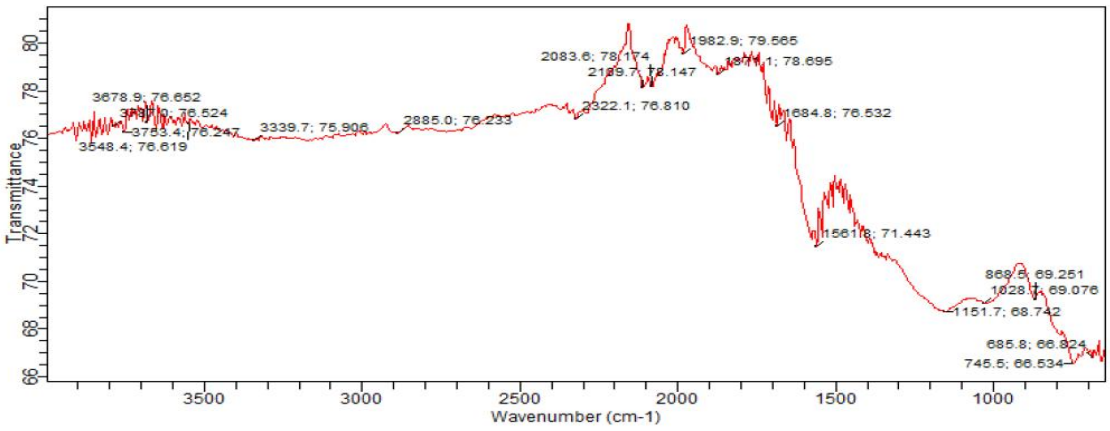

Figure 11: Fourier transform infrared (FTIR) for physically prepared *Cocos nucifera* shell catalyst

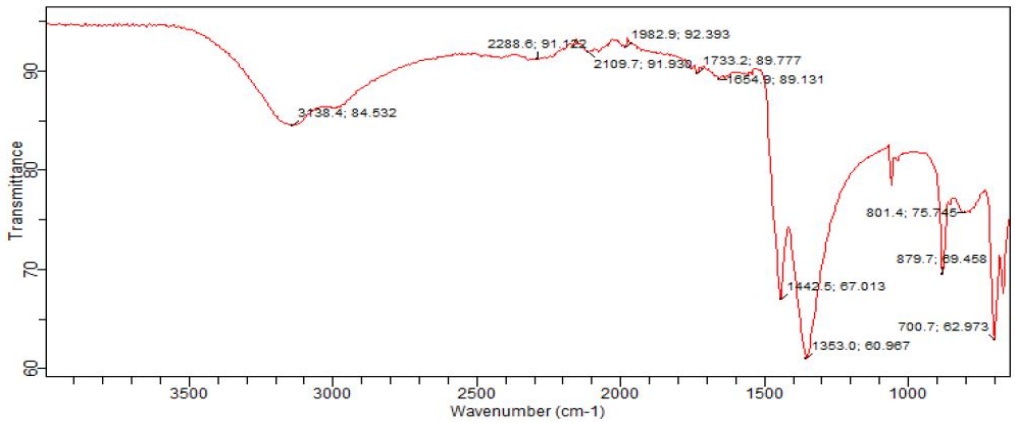

Figure 12: Fourier transform infrared (FTIR) for *Cocos nucifera* shell catalyst produced at 800°C

Micrograph Analysis of Catalyst Produced

The morphology of the catalyst was carried out using Scanning Electron Microscope. from the micrograph on Figure 13, the surface topography of catalyst produced by physical activation of *Cocos nucifera* shell showed different pores on the external surface of the catalyst. Figure 14, showed the types of different particles spread on the surface of the catalyst.

Base on the result of the morphology of catalyst produced by Physical activation of *Cocos nucifera* shell (Fig. 14), the external surface of the catalyst developed some crakes with some strands of crystals scattered on the surface of the catalyst. It also showed the type of particles present on the surface of the catalyst. The graph (Fig. 15) showed the cumulative (%) and volume (%) per area of the different particle per size. Due to carbonization and activation, volatiles and moisture content were removed producing a fixed carbon mass with widening of pore networks that are present in the catalyst sample which shows the adsorption capacity of a catalyst that largely depends on the number of pores and the size of the surface area. The physical activation process has successfully increased the surface area and porosity of the catalyst (Wang *et al*., 2013).

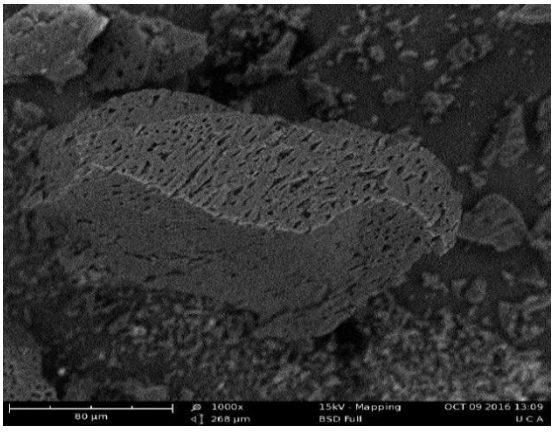

Figure 13: Morphology of catalyst produced by physical activation of Coconut shell

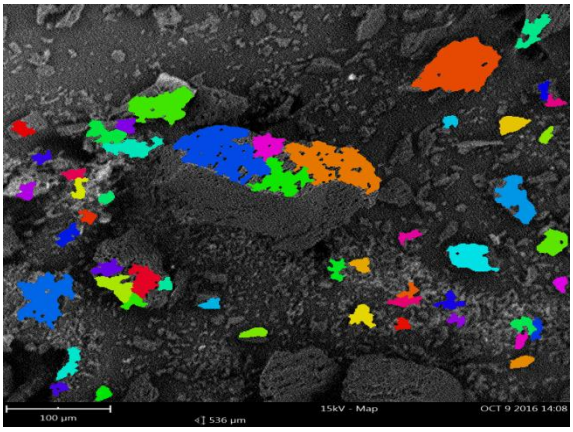

Figure 14: Types of different particles on of the catalyst produced by physical activation of Coconut shell

Figure 15. Graph of cumulative (%) against area of particles of catalyst produced by physical activation *Cocos nucifera* shell.

Conclusion

The heterogenous catalyst produced by physically activated *Cocos nucifera* shell has shown a good active site which can be used as catalyst for the production of biodiesel and other oil from plant seeds. This study serves as a tool to identify non-edible potential raw materials and to produce heterogeneous catalyst (AC supported on K_2CO_3) based on indigenous sourced raw materials for possible optimization of the bio-diesel production.

REFERENCES

Borel LDMS, De Lira TS, Ataíde CH. (2021). Thermochemical conversion of coconut waste: material characterization and identification of pyrolysis products. *Journal of Thermal Analysis and Calorimetry* 143: 637–646.

Charlotte Vogt and Bert M. Weckhuysen, (2022). The concept of active site in heterogeneous catalysis. *Nature Reviews Chemistry* volume 6, pages 89–111.

Dass PM, Louis H, Alheri A, Bifam M, and Ago MA. (2018). Production of Biodiesel Oil from Desert Dates (*Balanites aegyptiaca*) Seeds Oil Using a Heterogeneous Catalyst Produced from Mahogany (Khaya senegalensis) Fruit Shells. *Anal Chem Indian Journal*. 18(1):129.

Donni A., Wan M. A., Wan D. M., Kheireddline, A. (2005). Preparation and Characterization of Activated Carbon by Chemical Activation with K_2CO_3. *Journal of Bio-resource Technology* 98, 145-149.

Edward, M., Peter, O., Hillary, R. (2014). The Use of Impregnated Perlite as a Heterogeneous Catalyst for Biodiesel Production from Marula Oil. Chemical Papers-Slovak Academy of Sciences 68. (10), 234-240.

Eliseo Pascual, Lia Addadi, Mariano Andrés and Francisca Sivera, (2015). Mechanisms of crystal formation in gout—a structural approach. Nature Reviews Rheumatology volume 11, pages725–730.

Gao, L., Teng, G., Xiao, G.,Wei, R. (2010). Biodiesel from Palm Oil via Loading KF/Ca- Al-Hydrotalcite Catalyst. *Biomass and Bioenergy* vol. 34, pp 1283 1288.

Jiang C, Bo J and Xiao X, (2020). Converting waste lignin into nano-biochar as a renewable substitute of carbon black for reinforcing styrene-butadiene rubber. Waste Management 102: 732–742.

Kamaluddeen Suleiman Kabo, Abiodun B. Ogbesejana and Abdu Muhammad Bello (2020). Methanolysis of Balanite aegyptiaca (Desert Date) Oil using CaO as Catalyst. *chemSearch Journal* 11(1): 132 – 137.

Lee J, Sarmah AK, Kwon EE (2019) Production and formation of biochar. In: Yong SO, Bolan N, Tsang DCW, et al. (eds) *Biochar from Biomass and Waste: Fundamentals and Applications* (pp. 3–18). Amsterdam: Elsevier.

Li Y, Xing B, Ding Y, et al. (2020) A critical review of the production and advanced utilization of biochar via selective pyrolysis of lignocellulosic biomass. Bioresource Technology 312: 123614.

Sugumaran, P., Priya, S. V., Ravichandran, P. and Seshadri, S. (2012). Production and Characterization of Activated Carbon from Banana Empty Fruit Bunch and Delonix regia fruit Pod. *Journal of Sustainable Energy and Environment* 3, 125-132.

Verla, A. W., Horsfall, M (Jnr)., Verla, E.N., Spiff, A.I., Ekpete, O.A., (2012). Preparation and Characterization of Activated Carbon from Fluted Pumpkin (*Telfairia accidentalis* Hook. F) Seed Shell. *Asian Journal of Natural and Applied Sciences* vol. 1. (3), pp 39-50.

Wang, X.D., Li, J. W., Li, J.P., and Xia H (2013). Optimization of meso porous activated carbon from coconut shell by chemical activation with phosphoric acid. *Journal of Bio Resources.* 8, 6184-6195